Assessment of image quality for the new CT: Statistical reconstruction methods

Jeffrey A. Fessler

EECS Dept., BME Dept., Dept. of Radiology
University of Michigan

web.eecs.umich.edu/~fessler

AAPM: Interactive Session Imaging Scientific

July 30, 2012

1

Disclosure

- Research support from GE Healthcare
- Research support to GE Global Research
- Work supported in part by NIH grant R01-HL-098686
- Equipment support from Intel
- Research support from NIH (taxpayers)

2

Credits

Current (CT) students / post-docs
- Jang Hwan Cho
- Se Young Chun
- Donghwan Kim
- Jungkuk Kim
- Madison McGaffin
- Hung Nien
- Sathish Ramani
- Stephen Schmitt

GE collaborators
- Bruno De Man
- Jiang Hsieh
- Jean-Baptiste Thibault

CT collaborators
- Mitch Goodsitt, UM
- Ella Kazerooni, UM
- Neal Clinthorne, UM
- Paul Kinahan, UW

Former PhD students (who did/do CT)
- Yong Long, GE GRC
- Wonseok Huh, Bain & Company
- Hugo Shi, Continuum Analytics
- Joonki Noh, Emory
- Somesh Srivastava, GE HC
- Rongping Zeng, FDA
- Yingying, Zhang-O'Connor, RGM Advisors
- Matthew Jacobson, Xoran
- Sangtae Ahn, GE GRC
- Idris Elbakri, CancerCare / Univ. of Manitoba
- Saowapak Sotthivirat, NSTDA Thailand
- Web Stayman, JHU
- Feng Yu, Univ. Bristol
- Mehmet Yavuz, Qualcomm
- Hakan Erdoğan, Sabanci University

Former MS / undegraduate students
- Kevin Brown, Philips
- Meng Wu, Stanford
- ...

3

Qualitative comparison

Thin-slice FBP	ASIR image domain	Statistical (full MBIR)
Linear (mostly)	Nonlinear	Nonlinear

The nonlinear reconstructions appear to have "better" image quality...
Focus on MBIR methods because image-domain methods are a black-box...

4

Primary challenges for IQ assessment

- instrumentation (geometries)
- reconstruction methods *

Mathematical challenges
- Nonlinearity
- Nonstationarity (shift variance)

Practical challenges
- Relating mathematical characteristics to human observer performance
- ...

5

Sources of nonlinearity for FBP reconstruction

Physics effects
- Lambert-Beer law $e^{-\int \mu \, d\ell}$
- polyenergetic spectrum / beam hardening
- scatter
- logarithm

Usually these nonlinearities are handled as sinogram *preprocessing* steps.
(An exception is "iterative" beam-hardening correction for bone.)

Other nonlinearities
- Adaptive sinogram smoothing to reduce streaks
- Nonlinear post-processing (if any)
- Clamping (windowing) of image values for display
- Nonlinearity (gamma) of display device

6

Sources of nonstationarity for FBP reconstruction

- Heteroscedastic data statistics
- Divergent ray (cone-beam, fan-beam) geometries
- Irregular sampling patterns
  - cone-beam scanners, particularly with larger cone angles
  - dual-source CT with two different detector sizes
  - ...

Despite all these sources of nonlinearity and nonstationarity, traditional IQ measures like *local* MTF and *local* noise variance are useful for evaluating FBP reconstruction
(provided the preprocessing steps adequately handle the nonlinearities).

Now how about iterative methods?

7

MBIR reconstruction review

Penalized weighted least-squares (PWLS) cost function:

$$\hat{\boldsymbol{x}} = \arg\min_{\boldsymbol{x}} \Psi(\boldsymbol{x}), \quad \Psi(\boldsymbol{x}) = \frac{1}{2}\|\boldsymbol{y} - \boldsymbol{A}\boldsymbol{x}\|_{\boldsymbol{W}}^2 + \beta\,\mathrm{R}(\boldsymbol{x})$$

- $\boldsymbol{y}$: sinogram data, fully precorrected including logarithm
- $\boldsymbol{A}$: system matrix (forward projector)
- $\boldsymbol{W} = \mathrm{diag}\{w_i\}$: diagonal data-dependent statistical weighting matrix; ideally should account for all precorrection steps and both photon and electronic noise.
- β: regularization parameter, controls resolution/noise trade-off
- $\mathrm{R}(\boldsymbol{x})$: regularizer, often has the form $\mathrm{R}(\boldsymbol{x}) = \sum_k \psi([\boldsymbol{C}\boldsymbol{x}]_k)$ for some *potential function* ψ
- The "arg min" part requires an iterative optimization algorithm.
- Principles generalize to penalized-likelihood (Fessler, IEEE T-IP, Mar. 1996, Sep. 1996)

The "new" CT? Sauer & Bouman, IEEE T-SP, 1993.

8

New challenges for statistical image reconstruction

PWLS reconstruction: $\hat{\boldsymbol{x}} = \arg\min_{\boldsymbol{x} \succeq 0} \Psi(\boldsymbol{x}), \quad \Psi(\boldsymbol{x}) = \frac{1}{2}\|\boldsymbol{y} - \boldsymbol{A}\boldsymbol{x}\|_{\boldsymbol{W}}^2 + \beta\,\mathrm{R}(\boldsymbol{x})$

Q: Which of the following may cause nonlinear, shift-variant behavior?

1. Data-dependent weighting $\boldsymbol{W}$
2. Non-quadratic regularizers $\mathrm{R}(\boldsymbol{x})$
3. Nonnegativity constraints $\boldsymbol{x} \succeq \boldsymbol{0}$
4. Incomplete algorithm convergence "arg min"
5. All of the above

9

New challenges for statistical image reconstruction

PWLS reconstruction: $\hat{\boldsymbol{x}} = \arg\min_{\boldsymbol{x} \succeq \boldsymbol{0}} \Psi(\boldsymbol{x}), \quad \Psi(\boldsymbol{x}) = \frac{1}{2} \|\boldsymbol{y} - \boldsymbol{A}\boldsymbol{x}\|_{\boldsymbol{W}}^2 + \beta \, \mathrm{R}(\boldsymbol{x})$

Which of the following
may cause nonlinear, shift-variant behavior?

30% 1. Data-dependent weighting W
23% 2. Non-quadratic regularizers R
20% 3. Nonnegativity constraints
13% 4. Incomplete algorithm convergence
13% 5. All of the above

New challenges for statistical image reconstruction

PWLS reconstruction: $\hat{\boldsymbol{x}} = \arg\min_{\boldsymbol{x} \succeq \boldsymbol{0}} \Psi(\boldsymbol{x}), \quad \Psi(\boldsymbol{x}) = \frac{1}{2} \|\boldsymbol{y} - \boldsymbol{A}\boldsymbol{x}\|_{\boldsymbol{W}}^2 + \beta \, \mathrm{R}(\boldsymbol{x})$

Q: Which of the following may cause nonlinear, shift-variant behavior?

1. Data-dependent weighting $\boldsymbol{W}$
2. Non-quadratic regularizers $\mathrm{R}(\boldsymbol{x})$
3. Nonnegativity constraints $\boldsymbol{x} \succeq \boldsymbol{0}$
4. Incomplete algorithm convergence "arg min"
5. All of the above

All of the above, and more:

6. Non-quadratic log-likelihood for non-gaussian statistical models
7. Finite-precision effects in certain hardware implementations

10

Complications

Nonlinearity and nonstationarity complicate everything about IQ:

- resolution properties
  - local impulse response (point-spread function)
  - local modulation transfer function (MTF)
- noise properties
  - local variance
  - local autocorrelation function
  - local noise power spectrum
  - local distribution (*e.g.*, kurtosis)
  - "texture" of noise
- contrast properties (?)
- detection properties
  - analysis of model observers
  - empirical studies with human observers

11

Resolution properties: Local impulse response

$$\mathrm{LIR} \triangleq \frac{\hat{\boldsymbol{x}}(\boldsymbol{y}_{\text{with point}}) - \hat{\boldsymbol{x}}(\boldsymbol{y}_{\text{without point}})}{\text{amplitude of added point}}$$

The LIR of a statistical reconstruction methods depends on:

17% 1. Point location
20% 2. Point amplitude
13% 3. Surrounding object
30% 4. Data Statistics
20% 5. All of the above

Resolution properties: Local impulse response

$$\mathrm{LIR} \triangleq \frac{\hat{\boldsymbol{x}}(\boldsymbol{y}_{\text{with point}}) - \hat{\boldsymbol{x}}(\boldsymbol{y}_{\text{without point}})}{\text{amplitude of added point}}$$

Q: The LIR of a statistical reconstruction methods depends on:

1. Point location
2. Point amplitude (*cf.* linear reconstruction methods)
3. Surrounding object
4. Data statistics
5. All of the above

12

Resolution properties: Local impulse response

$$\mathrm{LIR} \triangleq \frac{\hat{\boldsymbol{x}}(\boldsymbol{y}_{\text{with point}}) - \hat{\boldsymbol{x}}(\boldsymbol{y}_{\text{without point}})}{\text{amplitude of added point}}$$

Q: The LIR of a statistical reconstruction methods depends on:

1. Point location
2. Point amplitude (*cf.* linear reconstruction methods)
3. Surrounding object
4. Data statistics
5. All of the above

All of the above, and more:

6. System model $\boldsymbol{A}$
7. Actual system response
8. Regularization method
9. Incomplete algorithm convergence

13

LIR example

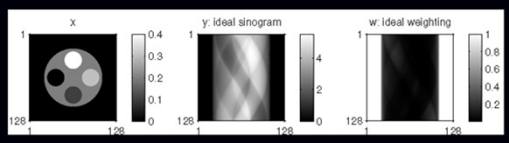

Q: How does FWHM of LIR for PWLS method compare at center of 4 disks?

1. same
2. higher attenuation disks have bigger FWHM (worse LIR)
3. lower attenuation disks have smaller FWHM (better LIR)
4. no relationship between attenuation and LIR
5. none of the above

14

LIR example

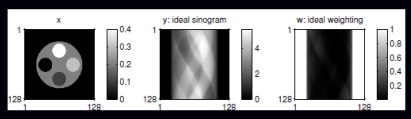

How does FWHM of LIR for PWLS method compare at center of 4 disks?

20% 1. same
20% 2. higher attenuation disks have bigger FWHM
17% 3. lower attenuation disks have smaller FWHM
30% 4. no relationship between attenuation and LIR
13% 5. none of the above

LIR example

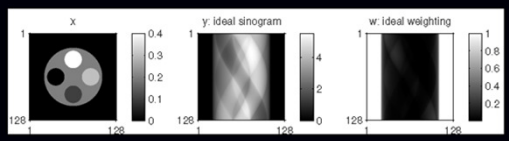

Q: How does FWHM of LIR for PWLS method compare at center of 4 disks?

1. same
2. higher attenuation disks have bigger FWHM (worse LIR)
3. lower attenuation disks have smaller FWHM (better LIR)
4. no relationship between attenuation and LIR
5. none of the above

None of the above.

- LIR *depends on the reconstruction method.*
- Likewise, the (local) MTF *depends on the reconstruction method.*

15

FHMW of LIR example

FWHM (angularly averaged) of LIR at center of each disk

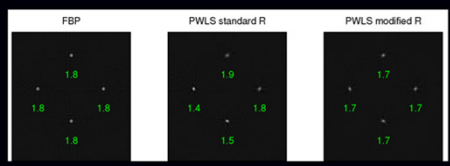

- Standard quadratic regularizer: differences between 8 neighboring pixels
- Modified quadratic regularizer: attempts to give uniform spatial resolution (Fessler & Rogers, IEEE T-IP, Sep. 1996)
- Other regularizers would induce yet different results
- Unweighted least squares with standard quadratic regularizer would be similar to FBP

16

Towards understanding LIR

Any "black box" algorithm can be studied empirically (*e.g.*, previous disk example).

Analysis can help obtain insight (*e.g.*, to help understand what results are generalizable).

PWLS $\hat{\boldsymbol{x}}$ is not only a *nonlinear* function of the (precorrected) data $\boldsymbol{y}$:

$$\hat{\boldsymbol{x}} = \arg\min_{\boldsymbol{x} \geq 0} \Psi(\boldsymbol{x}), \quad \Psi(\boldsymbol{x}) = \frac{1}{2} \|\boldsymbol{y} - \boldsymbol{A}\boldsymbol{x}\|_{\boldsymbol{W}}^2 + \beta \, \mathrm{R}(\boldsymbol{x}),$$

$\hat{\boldsymbol{x}}$ is defined *implicitly* in terms of $\boldsymbol{y}$, complicating analysis.

To simplify analysis:

- Focus on case where algorithm is iterated "to convergence." Eliminates the iterative algorithm from consideration. Only Ψ matters.
- Ignore the nonnegativity constraint (which is quite nonlinear). (It mainly affects background air regions for well regularized cases.)

- Look at the limit of a low-contrast point source (low-contrast case)

17

LIR expression for PWLS

The LIR at the jth voxel is (Fessler & Rogers, IEEE T-IP, Sep. 1996):

$$\mathrm{LIR}_j = \left[\boldsymbol{A}'\boldsymbol{W}\boldsymbol{A} + \beta \nabla^2 \mathrm{R}(\boldsymbol{x})\right]^{-1} \boldsymbol{A}'\boldsymbol{W}\boldsymbol{A}_{\mathrm{true}} \boldsymbol{e}_j$$

LIR depends on:

- point location j
- type of regularizer through its Hessian $\nabla^2 \mathrm{R}$
- surrounding object $\boldsymbol{x}$ (for non-quadratic regularizers)
- data statistics $\boldsymbol{W}$
- true system response $\boldsymbol{A}_{\mathrm{true}}$ and system model $\boldsymbol{A}$

Using this analysis, we can design regularizer $\mathrm{R}(\boldsymbol{x})$ to guide spatial resolution properties, *e.g.*, make resolution approximately uniform and isotropic, and largely independent of the object and statistics, at least for quadratic regularizers.

(Stayman & Fessler, IEEE T-MI, 2000, 2001, 2004)

However, uniform spatial resolution usually means nonuniform noise in CT. (probably always)

18

Noise maps for PWLS image reconstruction

CT simulation with XCAT phantom:

Q: For PWLS reconstruction, compared to the noise variance of $\hat{x}$ in the heart region, the noise variance in the lung region is:

1. Much lower
2. Somewhat lower
3. Comparable
4. Higher
5. None of the above

19

Noise maps for PWLS image reconstruction

CT simulation with XCAT phantom:

For PWLS reconstruction,
compared to the noise variance in the heart region,
the noise variance in the lung region is:

17%	1. Much lower
17%	2. Somewhat lower
17%	3. Comparable
30%	4. Higher
20%	5. None of the above

Noise maps for PWLS image reconstruction

CT simulation with XCAT phantom:

Q: For PWLS reconstruction, compared to the noise variance of $\hat{x}$ in the heart region, the noise variance in the lung region is:

1. Much lower
2. Somewhat lower
3. Comparable
4. Higher
5. None of the above

None of the above.
Noise properties depend on reconstruction method ($\boldsymbol{A}$, $\boldsymbol{W}$, R, ...).

20

Empirical noise maps for PWLS image reconstruction

CT simulation with XCAT phantom:

standard regularizer:

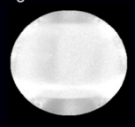

"uniform resolution" regularizer:

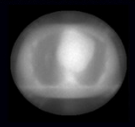

These are both results from simple *quadratic* regularizers.
Edge-preserving regularizers produce more variable noise maps.

(Zhang-O'Connor & Fessler, IEEE T-MI, 2007)

21

Predicting noise properties

For PWLS with quadratic regularization: (Fessler, IEEE T-IP, Mar. 1996)

$$\mathrm{Cov}\{\hat{x}\} \approx \left[\boldsymbol{A}'\boldsymbol{W}\boldsymbol{A} + \beta\nabla^2\mathrm{R}\right]^{-1}\boldsymbol{A}'\mathrm{Cov}\{y\}\boldsymbol{A}\left[\boldsymbol{A}'\boldsymbol{W}\boldsymbol{A} + \beta\nabla^2\mathrm{R}\right]^{-1}$$

Useful for predicting:

- *local* reconstructed image variance
- *local* image autocorrelation
- *local* noise power spectrum

Empirical:

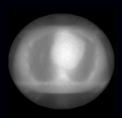

Predicted:

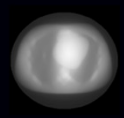

In principle can use such noise predictions to inform regularization design and selection of regularization parameter β.
Unfortunately, analysis for *non-quadratic* regularization is very difficult.
For TV and l_1-based sparsity regularizers even harder.

22

Empirical noise properties: Kurtosis

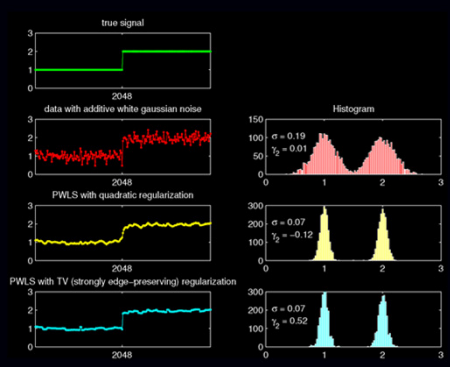

23

Kurtosis continued

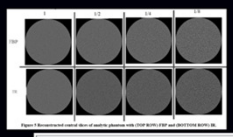

(Pachon *et al.*, SPIE 2012)

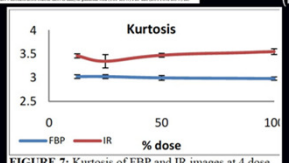

FIGURE 7: Kurtosis of FBP and IR images at 4 dose levels. The higher kurtosis of IR images indicates that the noise distribution in these images slightly deviates from a normal distribution (excess factor −0.5) .

Q: "IR" ?

For non-Gaussian images, second moments (NPS) are an incomplete story.

24

Contrast-dependent edge resolution: 1D

Orig:

Noiseless blurry image:

Restored image using PWLS $\delta = 1$:

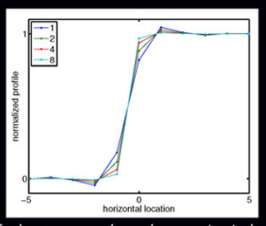

Challenge: *Shape of edge response depends on contrast when "preserving edges."*

25

Contrast-dependent edge resolution: 2D CT

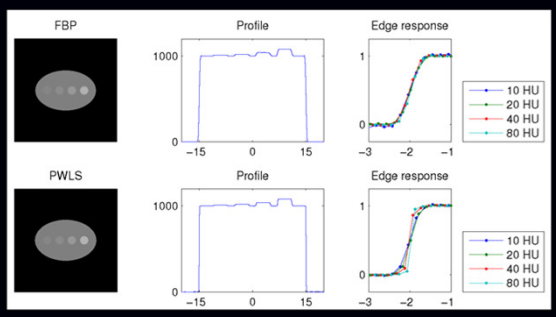

Challenge:
Shape of edge response depends on contrast for edge-preserving regularization.

26

Contrast-dependent MTF

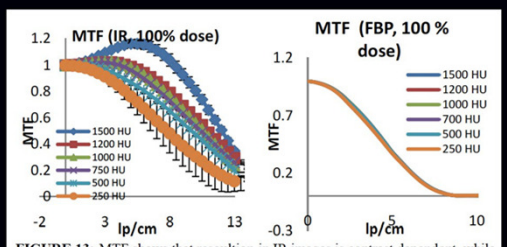

FIGURE 13: MTF shows that resoultion in IR images is contrast dependent, while MTF of FBP images is independent of contrast.

(Pachon *et al.*, SPIE 2012) "IR" ?

See Evans *et al.*, Med. Phys., Mar. 2011 for more contrast-dependent effects (on noise-resolution trade-off) for a penalized-likelihood method with log-cosh edge-preserving regularizers.

27

Optimizing regularizers for signal detection

SNR of channelized Hotelling observer (CHO)
for signal-known-exactly (SKE) task,
applied to PWLS reconstruction with quadratic regularizer.

Q: How much does regularization ($\beta > 0$) improve SNR over $\beta = 0$?

1. A lot, if we select proper β
2. At best only a little
3. Makes no difference
4. Quadratic regularization degrades SNR due to blur

28

Optimizing regularizers for signal detection

SNR of channelized Hotelling observer (CHO)
for signal-known-exactly (SKE) task,
applied to PWLS reconstruction with quadratic regularizer.

How much does (quadratic) regularization improve SNR of CHO for SKE detection task?

33%	1. A lot, if we select proper beta
23%	2. At best only a little
27%	3. Makes no difference
17%	4. Quadratic regularization degrades SNR (due to blur)

Optimizing regularizers for signal detection

SNR of channelized Hotelling observer (CHO)
for signal-known-exactly (SKE) task,
applied to PWLS reconstruction with quadratic regularizer.

Q: How much does regularization ($\beta > 0$) improve SNR over $\beta = 0$?

1. A lot, if we select proper β
2. At best only a little
3. Makes no difference
4. Quadratic regularization degrades SNR due to blur

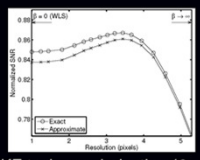

(Yendiki & Fessler, IEEE T-MI, Jan. 2006)

For SKE task, regularization ($\beta > 0$) improves SNR only a little over $\beta = 0$.

29

Choosing β: Unknown location

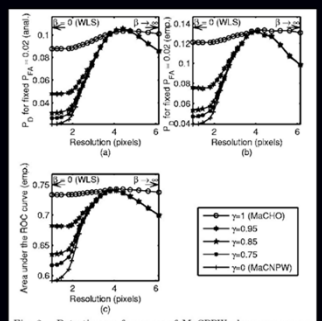

Fig. 2. Detection performance of MaCPPW observers versus QPWLS reconstruction resolution: P_D obtained analytically (a), P_D obtained empirically (b), and AUC obtained empirically (c). Results are shown for five different degrees of prewhitening accuracy. The search area is a disk with a diameter of 9 pixels.

AUC for signal detection with unknown location task.

Benefits of β depend on ability of observer to prewhiten.

(Yendiki & Fessler, JOSA-A 24(12):B199, Dec. 2007)

30

Other complications

- 3D regularization (vs FBP)
- temporal / dynamic CT reconstruction (inherently missing data)
- dual-energy, dual-source, ...
- ...

31

Summary

- For quadratic regularization we have good understanding of local resolution and noise properties.
- Nonquadratic case is less well understood, though progress has been made for smooth edge-preserving regularizers:
  Ahn & Leahy, IEEE T-MI, Mar. 2008
  Non-smooth regularizers like TV and l_1 are wide open problems.

Take aways

- Resolution/noise properties *depend on the reconstruction method* including all of its specific models and components (*e.g.*, regularizer)
- Report *local* LIR/PSF and *local* MTF and *local* NPS.
- Focus on low-contrast signals for comparing FBP vs "IR"
- Include unknown location tasks in IQ assessment
- Be wary of general claims about
  "statistical image reconstruction methods" vs FBP
- When publishing (or reviewing) comparisons, provide (or require) a description of the statistical image reconstruction method.

32

Bibliography

[1] J-B. Thibault, K. Sauer, C. Bouman, and J. Hsieh. A three-dimensional statistical approach to improved image quality for multi-slice helical CT. *Med. Phys.*, 34(11):4526–44, November 2007.

[2] J. A. Fessler and W. L. Rogers. Spatial resolution properties of penalized-likelihood image reconstruction methods: Space-invariant tomographs. *IEEE Trans. Im. Proc.*, 5(9):1346–58, September 1996.

[3] J. A. Fessler. Mean and variance of implicitly defined biased estimators (such as penalized maximum likelihood): Applications to tomography. *IEEE Trans. Im. Proc.*, 5(3):493–506, March 1996.

[4] K. Sauer and C. Bouman. A local update strategy for iterative reconstruction from projections. *IEEE Trans. Sig. Proc.*, 41(2):534–48, February 1993.

[5] J. W. Stayman and J. A. Fessler. Regularization for uniform spatial resolution properties in penalized-likelihood image reconstruction. *IEEE Trans. Med. Imag.*, 19(6):601–15, June 2000.

[6] J. W. Stayman and J. A. Fessler. Nonnegative definite quadratic penalty design for penalized-likelihood reconstruction. In *Proc. IEEE Nuc. Sci. Symp. Med. Im. Conf.*, volume 2, pages 1060–3, 2001.

[7] J. W. Stayman and J. A. Fessler. Compensation for nonuniform resolution using penalized-likelihood reconstruction in space-variant imaging systems. *IEEE Trans. Med. Imag.*, 23(3):269–84, March 2004.

[8] Y. Zhang-O'Connor and J. A. Fessler. Fast predictions of variance images for fan-beam transmission tomography with quadratic regularization. *IEEE Trans. Med. Imag.*, 26(3):335–46, March 2007.

[9] J. H. Pachon, G. Yadava, D. Pal, and J. Hsieh. Image quality evaluation of iterative CT reconstruction algorithms: a perspective from spatial domain noise texture measures. In *Proc. SPIE Medical Imaging 2012: Phys. Med. Im.*, page 83132K, 2012.

[10] J. D. Evans, D. G. Politte, B. R. Whiting, J. A. O'Sullivan, and J. F. Williamson. Noise-resolution tradeoffs in x-ray CT imaging: A comparison of penalized alternating minimization and filtered backprojection algorithms. *Med. Phys.*, 38(3):1444–58, March 2011.

[11] A. Yendiki and J. A. Fessler. Analysis of observer performance in known-location tasks for tomographic image reconstruction. *IEEE Trans. Med. Imag.*, 25(1):28–41, January 2006.

[12] S. Ahn and R. M. Leahy. Analysis of resolution and noise properties of nonquadratically regularized image reconstruction methods for PET. *IEEE Trans. Med. Imag.*, 27(3):413–24, March 2008.

33